Journal of Additive Manufacturing Technologies
DOI: 10.18416/JAMTECH.24121156

Infinite Science | Publishing

Localization of Acoustical Events in Laser Metal Deposition

J. U. Weber[1*], N. Hoffmann[1] and C. Emmelmann[2]

[1] *Fraunhofer Research Institution for Additive Manufacturing Technologies IAPT, Hamburg, Germany*
[2] *Institute of Laser and System Technologies (iLAS), Hamburg, Germany*
[*] *Corresponding author, email: julian.ulrich.weber@iapt.fraunhofer.de*

Abstract

Laser Metal Deposition (LMD) combines laser energy and powder material to create complex structures on existing components. It enables cost-effective production of multi-material compositions, like reinforcing metals with ceramic particles for enhanced wear resistance. However, dissimilar material characteristics can lead to defects, especially crack propagation and delamination. Efforts focus on optimizing process parameters and real-time monitoring to reduce the effort of mitigating defects. Assessing acoustic emissions aids in early defect detection and provides process stability insights. Besides of time- and frequency resolved information on the acoustical signals, precise defect localization is crucial, especially for manufacturing programs with multiple components on a substrate material. To instantly locate delamination defects, a multi-microphone array is proposed. This study also explores localization techniques, accuracy, and reliability. To investigate these, experiments on a test platform were used with simulated acoustical events that replicate known defect sounds.

Keywords: LMD, Process Monitoring, Acoustical Monitoring, Localization.

1. Introduction

Laser Metal Deposition (LMD) is a type of Additive Manufacturing (AM) processes, that can be utilized to generate complex structures on existing parts or deposit functional material structures on dissimilar substrate materials. It allows the deposition of shape memory alloy structures or material compounds with improved hardness on standard substrate materials, however the bonding process suffers due to differing material properties. Crack propagation and delamination in the bonding zone are common defects [1, 2].

To identify and analyze critical defects early, audio emission (AE) monitoring is suitable approach. Conventional time- and frequency-resolved AE analysis can be used to identify and characterize acoustical events in time and frequency. However, it fails to disclose essential details regarding the precise AE source location.

AE localization, especially crack-propagation is well researched in civil engineering applications, such as structural health monitoring in beams or manufacturing of large plate like materials. Most of the localization research focusses on structure-born audio emission monitoring in larger environments [3, 4]. First localization approaches in AM were promising for related Powder-Bed Fusion processes using laser and metal powder (PBF-LB/M) by means of structural-borne emission monitoring. Here, localization was performed with two contact-based sensors, a localization accuracy of 3 mm was reached [5]. However, the use of a microphone array to monitor and localize airborne audio emissions offers higher flexibility and less installation effort. This approach within the LMD environment is not researched yet and therefore focus of this study.

A concept of a multi-microphone array to monitor and localize airborne AE two-dimensionally in small manufacturing dimensions is used, with a monitoring area of up to 500 x 500 mm.

2. Material and methods

In this study, modelled audio signals, derived from original LMD experiment data, were employed for audio localization. LMD was conducted using a Nd:YAG laser (wavelength: 1070 nm) with Argon gas for shielding and carrier purposes (average flow rate: 5 l/min) to maintain a residual O_2 concentration of about 200 ppm in the process chamber. Powder flow was regulated by a disk-conveying system. Two types of powders, pre-alloyed NiTi and an in-situ mixed composite of 316L and SiC, were used, along with Ti and 316L substrates. As expected, crack propagation and delamination were observed during the process. Acoustic signals were captured using a directional microphone (Sennheiser MKE 600) and processed by an audio interface (Behringer U-Phoria UMC202HD) with a maximum sample rate of 96 kHz. Prior analyses revealed that pertinent transient audio events exhibited peaks within a frequency range of 4 to 15 kHz, with peak agglomeration at 12 kHz.

The targeted audio signal (transient cracking sound in 12 kHz) was then replicated via an omni-directional speaker for simplified localization experiments. A multi-microphone array, consisting of up to six microphones with various audio interface configurations, was assembled. The choice of audio hardware was driven by a cost-effective approach for monitoring systems. Three primary experimental setups are illustrated in Fig. 1 and were conducted for 1D-localization experiments.

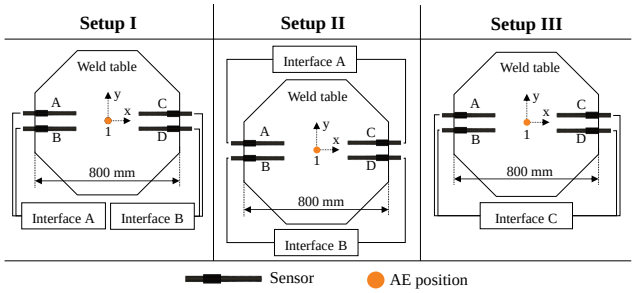

Fig 1. 1D experimental setup I – III for investigation of localization parameters.

The sensor and audio emission positions are summarized in Tab. 1.

Various experiments were conducted to study localization parameters, influencing factors, and setup configurations. In 1D-localization experiments, four microphones were utilized with single or dual audio interfaces. The focus of setup I, II and III was to investigate the influence of audio interface types and sensor connection variations. Interface A and B represent audio interfaces, to convert an analog signal to a digital signal. Each interface has two input channels to acquire analog signals, therefore two identical interfaces had to be utilized to convert four signals. Interface C is a single interface with up to eight input channels. After identification of ideal setup configuration (interface type, sensor connection pattern, filter parameters), experimental data was used to identify a suitable algorithm, to calculate the Time Difference of Arrival (TDOA). Signals were visualized using Python and MATLAB libraries (Numpy, pywt, SciPy). To determine Time Difference of Arrival (TDOA), one sensor signal was held constant while the corresponding signal was manually and automatically shifted in the time domain. This shift continued until the smallest signal discrepancy was identified. The smallest signal discrepancy, here defined as $n_{t,s}$, was ascertained by means of cross-correlation, least difference, and least squared difference. The shift $n_{t,s}$ is calculated by analysing the following function:

$$f(n_{t,s}) = \sum_{i=imin}^{imax} (S_{a,i} - S_{c,(i+n_{t,s})})^2 \quad (1)$$

The function is based on the least square method, where S_a and S_c are referring to the time-resolved signal of sensor A and C; indices i_{min} and i_{max} are boundaries of a band, derived by threshold T. At T, the signal A surpasses a pre-defined signal amplitude for the first time. Finding the minima of (1) delivers the smallest signal difference between signal A and C. The unitless value $n_{t,s}$ can be converted to the distance between two signals A and C by equation (2), where c_s is the propagation speed and f_s is the used sample rate.

$$d_{s,A,C} = \frac{n_{t,s,A,C}}{f_s} c_s \quad (2)$$

For every 1D-experiment with 4 sensors (A, B, C, D), 6 signal difference values (comparison of A → B; A → C; A → D; B → C; B → D) were calculated. After completion of all testing series, mean values were calculated based on the absolute offsets to the expected signal difference values. Six testing series were conducted for every setup.

Further, two setups were investigated for 2D-localization experiments, illustrated in Fig. 2.

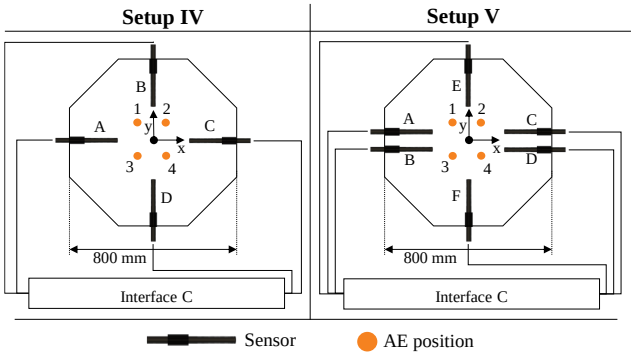

Fig 2. 2D experimental setup IV – V for validation of localization parameters.

After identification of all relevant parameters, 2D-localization experiments were conducted to validate the setup configuration. Sensor pairs, aligned along the same axis, were employed to compute relative audio emission locations for each dimension. Within x-y plane, the distance between signal S and sensor A is defined by equation (3) and for sensor C in (4).

$$d(\vec{S}, \vec{A}) = \sqrt{(A_x - S_x)^2 + (A_y - S_y)^2} \quad (3)$$

$$d(\vec{S}, \vec{C}) = \sqrt{(C_x - S_x)^2 + (C_y - S_y)^2} \quad (4)$$

Subtracting (3) and (4) delivers the relative distance shift between both sensors A and C and signal S, $d_{s,A,C}$.

$$d_{s,A,C} = d(\vec{S}, \vec{A}) - d(\vec{S}, \vec{C}) \quad (5)$$

(2) and (5) can be equated rearranged to S_y, which delivers the function g with the variables $n_{t,s}$ and S_x:

$$S_y = g(n_{t,s}, S_x) \quad (6)$$

Therefore, to identify the x- and y-coordinate of the AE

source, function (6) has to be computed for two independent sensor pairs, delivering two functions. The intersection of both functions delivers the coordinates of the AE source. Thus, at least 3 sensors are necessary to localize the AE source.

Table 1. Overview of Audio Emission (AE) and sensor positions for all experiments.

	Position	x-coordinate	y-coordinate
Setup I - III	AE pos. 1	0	0
	Sensor A	-340	70
	Sensor B	-340	-70
	Sensor C	340	70
	Sensor D	340	-70
Setup IV	AE pos. 1	-75	75
	AE pos. 2	75	75
	AE pos. 3	-75	-75
	AE pos. 4	75	-75
	Sensor A	-340	0
	Sensor B	0	340
	Sensor C	340	0
	Sensor D	0	-340
Setup V	AE pos. 1	-75	75
	AE pos. 2	75	75
	AE pos. 3	-75	-75
	AE pos. 4	75	-75
	Sensor A	-340	70
	Sensor B	-340	-70
	Sensor C	340	70
	Sensor D	340	-70
	Sensor E	0	340
	Sensor F	0	-340

3. Results and discussion

To identify the most suitable setup for 1D-localization, 6 testing series were conducted for each setup (I – III). The signal difference values were calculated by means of least squared difference algorithm. A 2nd order butterworth filter with lower cut-off frequency of 10 kHz and a higher cut-off frequency of 14 kHz was used, to focus all relevant frequency around 12 kHz. A high sensitivity to filter parameters was observed, therefore filter parameters were held constant for all experiments. Due to an equidistant, centered position of the AE source (AE pos. 1), no signal difference is expected between the sensor pairs. The resulting mean offset data is summarized in form of triangular matrices in Table 2.

The results show best performance in setup III. The mean measured offset of sensor pairs in setup 1 range between 4,72 and 80 samples. The calculated offsets for sensor pairs A → B and C → D yield a much lower offset compared to A → C and B → D. The same image is drawn for setup II, where calculated signal difference values for sensor pairs A → C and B → D are much lower than A → B and C → D.

Table 2. Overview of mean signal difference values for all 1D localization experiments.

	A	B	C	D	Description
A	-	0	0	0	Signal difference values n_{ts} (expected)
B		-	0	0	
C			-	0	
D				-	
A	-	4.72	80	67.8	Mean signal difference values $n_{ts,I}$ (Setup I)
B		-	60.4	78.6	
C			-	4.72	
D				-	
A	-	31.2	11.8	42	Mean signal difference values $n_{ts,II}$ (Setup II)
B		-	42.8	15.2	
C			-	31	
D				-	
A	-	3.17	1.5	6.16	Mean signal difference values $n_{ts,III}$ (Setup III)
B		-	5.5	6.17	
C			-	0.67	
D				-	

The high difference results in the use of two separate audio interfaces and states, that localization tasks require a single audio interface respectively a single analog-digital converter (AD-C) for all utilized sensors. The tested equipment configured as setup III, yields an offset of mean signal difference values between 0.67 – 6.17 time samples, resulting in a 1D localization accuracy of at least 22 mm. With a sample rate of 96 kHz and propagation velocity of sound of 343.2 m/s, a single time sample shift equals 3.58 mm of geometrical shift.

To evaluate the influence of the algorithms that are used to calculate the TDOA, the data set of setup III was used. $N_{t,s}$ were calculated by means of (i) normalized cross-correlation, (ii) value difference method, (iii) value difference squared method and (iv) threshold method. All filter and peak parameters were held constant. All values were compared to the expected signal discrepancies (0 matrix) and are summarized in

Table 3 as mean offset signal difference values.

The value difference squared method can be identified as most favourable algorithm to calculate $n_{t,s}$. However, the results of normalized cross-correlation and difference values also show robust results. For the threshold-based method, three outliers can be identified, signalising a fragile performance for transient signal comparison, such as defect events in LMD.

Table 3. Influence of signal comparison algorithms.

	A	B	C	D	Description
A	-	3.17	3.17	6.16	Mean signal difference values $n_{ts,NCC}$ by (i) Normalized cross-correlation
B		-	5.5	6.17	
C			-	0.67	
D				-	
A	-	6.17	3.17	6.17	Mean signal difference values $n_{ts,D}$ by (ii) value difference method
B		-	10.51	7.34	
C			-	2.0	
D				-	
A	-	3.17	1.5	6.16	Mean signal difference values $n_{ts,DS}$ by (iii) value difference squared method
B		-	5.5	6.17	
C			-	0.67	
D				-	
A	-	19275	3.5	3	Mean signal difference values $n_{ts,T}$ by (iv) threshold method
B		-	19272	19272	
C			-	0.5	
D				-	

Based on the results, all other experiments utilized the value difference squared method. 2D-localization experiments were conducted by use of setup IV and setup V. For each AE position, three independent data sets were acquired. Localization results are shown in Fig 3 for setup IV and Fig 4 for setup V.

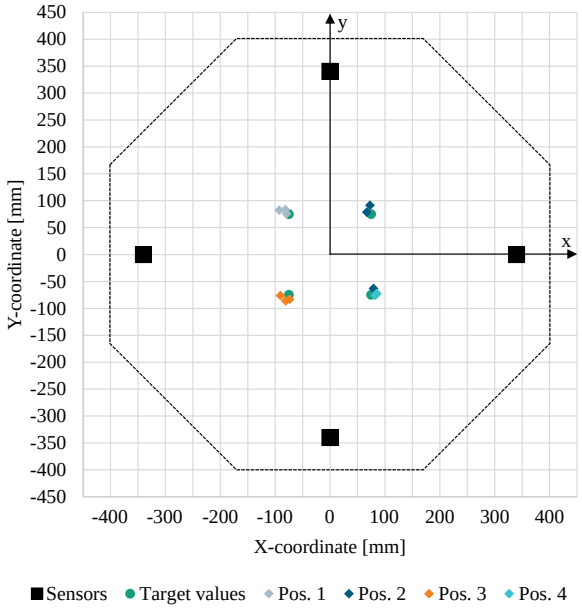

Fig 3. Localization results of setup IV.

The graphical visualization in shows good localization results for both setups. Most calculated localization values can be found within the square of the targeted values in the data grid (50 mm × 50 mm). For setup IV, Pos. 2, one strong measured outlier can be identified. The measured value can be found in the area of the targeted value of Pos. 4. Further for setup IV, stronger scattering of measured data points can be identified for values of Pos. 4. Manual analysis of the corresponding recorded data show, that the recording quality of one sensor was comparably low, resulting in a miscalculation of time shifts between two signals. The effect is visualized by plotting four signals of two sensor pairs, where one pair contains two high quality data set and the other pair contains one high and one lower quality data set. The signals plots are shown in Fig 5.

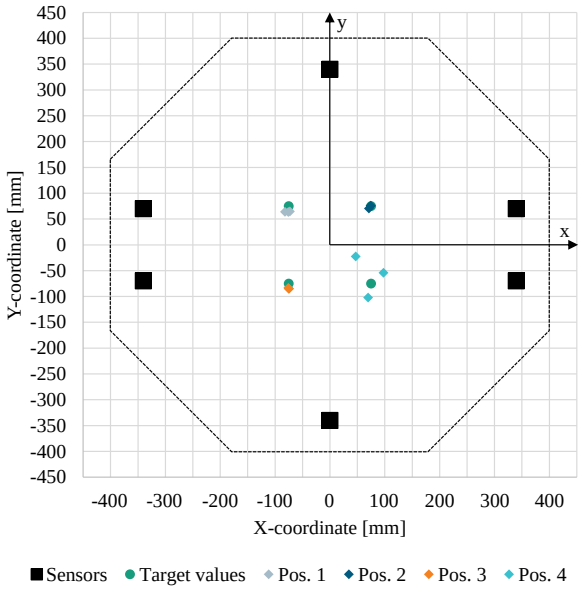

Fig 4. Localization results of setup V.

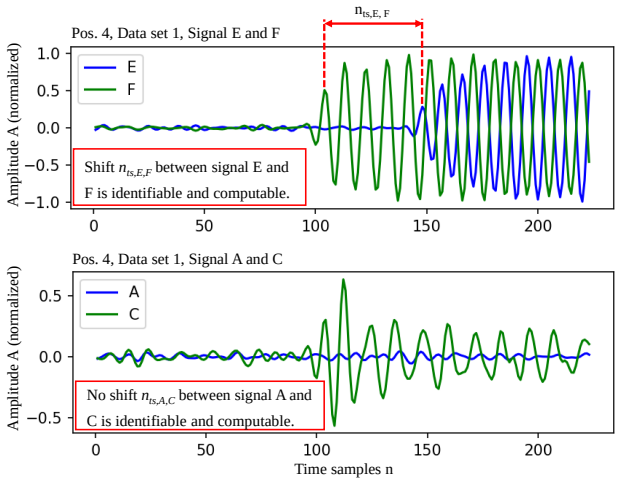

Fig 5. Signal data comparison of sensor pair E-F (top) and A-C (bottom) visualizes the influence of low quality data recordings (bottom) on identification of smallest signal difference n_{ts}.

Further quantitative evaluation requires the analysis of mean values (*MV*), target values (*TV*), standard deviation (*SD*), mean absolute error (*MAE*) and mean relative error (*MRE*). All values are summarized in Table 4 below.

The numerical data also shows significant outliers in Pos. 2 (Setup IV) and Pos. 4 (Setup V). The reason for these outliers are low quality data sets due to defective sensors, as described above. Thus, further performance

analysis doesn't include data of setup IV, Pos. 2 and setup V, Pos. 4.

Table 4. Summary of 2D localization results for both setups (IV and V).

	Pos.	Dim.	MV [mm]	SD [mm]	MAE [mm]	MRE [%]
Setup IV	1	X	-84.39	5.69	9.39	13
		Y	80.45	3.38	5.45	7
		$(x^2+y^2)^{1/2}$	-	6.62	10.85	-
	2	X	73.11	4.90	1.89	3
		Y	35.55	70.00	39.45	53
		$(x^2+y^2)^{1/2}$	-	70.17	39.49	-
	3	X	-81.56	6.89	6.56	9
		Y	-81.90	4.14	6.90	9
		$(x^2+y^2)^{1/2}$	-	8.03	9.52	-
	4	X	84.07	1.48	9.07	12
		Y	-73.71	1.59	1.29	2
		$(x^2+y^2)^{1/2}$	-	2.18	9.16	-
Setup V	1	X	-76.89	3.79	1.89	3
		Y	63.83	0.42	11.17	15
		$(x^2+y^2)^{1/2}$	-	3.81	11.33	-
	2	X	73.39	1.58	1.64	2
		Y	73.79	2.53	1.21	2
		$(x^2+y^2)^{1/2}$	-	2.98	2.04	-
	3	X	-74.90	0.52	0.10	0
		Y	-84.55	0.77	9.55	13
		$(x^2+y^2)^{1/2}$	-	0.93	9.55	-
	4	X	71.53	20.61	3.47	5
		Y	-59.65	32.59	15.35	20
		$(x^2+y^2)^{1/2}$	-	38.56	15.74	-

For Setup IV, a SD between 1.46 and 6.89 mm, one-dimensional MAE between 1.29 and 9.39 mm and MRE between 2 and 13 % can be reached. Across all measuring positions, a two-dimensional MAE ($(x^2+y^2)^{1/2}$) of 9.85 mm is achieved. Setup V yields comparable results with a SD between 0.42 and 3.79 mm, MAE between 0.10 and 11.17 mm and MRE between 2 and 15 %. The magnitude of all MAE in two dimensions for setup V is 7.64 mm. Therefore, the SD is significantly lower for setup V compared to setup IV, indicating a more robust measurement with an increasing number of sensors. However, the overall error is slightly higher in setup V. Together with the lower scattering of measured data (as seen in decreased SD), the slightly higher MAE and MRE are an implication for a systematic measurement error, which could be decreased with a calibration process. However, the higher mean error in setup V is only valid for the y-dimension. Setup V includes two additional sensors in x-dimension. In x-dimension, setup V yields a MAE between 0.10 and 3.47 mm, which is significantly improved, compared to setup IV. These results indicate an improved robustness and accuracy by the addition of further sensors, referred to 1D-localization.

Significant differences between the measuring positions are not identifiable.

4. Conclusions

This study explored a multi-microphone array for localizing specific audio emissions associated with critical defect formation in LMD manufacturing. Sensitivity to influencing factors (filtering, system setup, and localization algorithms) was observed across a range of levels. The study achieved a high localization accuracy and noted enhanced reproducibility with an increased number of microphones. The following conclusions can be drawn from 1D and 2D localization experiments

- Dependency on hardware setup: Audio signal localization only works reliable with a single analog-digital converter (audio interface). Multiple interfaces require digital synchronization.
- Filtering of the signal is necessary; however, localization can suffer from unsuitable filter parameters.
- Accuracy is limited by the minimum time step of microphone and audio interface, therefore defined by the systems sample rate.
- Best results are achieved by use of value difference squared method to calculated the time shifts between to sensor signals.
- Four different AE positions were identified within an x-y-plane, a mean absolute error of 7.63 mm was reached for the setup with 6 sensors. Increased robustness and accuracy are reached after adding additional sensors to a measurement dimension.

This work investigates only a few of many influencing factors on the localization performance and is only valid for the presented monitoring setup. A transfer to similar systems requires further setup and calibration efforts. Future efforts will focus on augmenting the microphone array and implementing in-process localization within the LMD process.

Acknowledgments
Part of this work was funded by the Federal Ministry of Education and Research (BMBF) of the Federal Republic of Germany within the FAMILIAR project (01IS22031B).

Author's statement
Conflict of interest: Authors state no conflict of interest. Informed consent: Informed consent has been obtained from all individuals included in this study. Ethical approval: The research related to human use complies with all the relevant national regulations, institutional policies and was performed in accordance with the tenets of the Helsinki Declaration, and has been approved by the authors' institutional review board or equivalent committee.

References

[1] T. Hauser, R. T. Reisch, T. Kamps, A. F. H. Kaplan und J. Volpp, "Acoustic emissions in directed energy deposition processes", *Int J Adv Manuf Technol*, 2022.

[2] J. U. Weber, M. Knabe, V. Sayilgan und C. Emmelmann, "Signal processing of airborne acoustic emissions from laser metal deposited structures", *Procedia CIRP*, Jg. 111, S. 359–362, 2022.

[3] F. Zhang, L. Pahlavan und Y. Yang, "Evaluation of acoustic emission source localization accuracy in concrete structures", *Structural Health Monitoring*, Jg. 19, Nr. 6, S. 2063–2074, 2020.

[4] M. U. Liaquat, H. S. Munawar, A. Rahman, Z. Qadir, A. Z. Kouzani und M. A. P. Mahmud, "Localization of Sound Sources: A Systematic Review", *Energies*, Jg. 14, Nr. 13, S. 3910, 2021.

[5] K. Ito, M. Kusano, M. Demura und M. Watanabe, "Detection and location of microdefects during selective laser melting by wireless acoustic emission measurement", *Additive Manufacturing*, Jg. 40, S. 101915, 2021.